A DESIGN MODEL FOR SURFACE TERMINATION PROFILE OPTIMISATION OF P-N JUNCTIONS

J. B. Waddell and J. Middleton

Department of Civil Engineering, University College of Swansea
Singleton Park, Swansea SA2 8PP, U.K.

1. Summary

This paper presents the development of a design model for the evaluation of an optimal surface termination profile for off-state semiconductor problems. The finite element method is used in the analysis phase and a moving mesh technique using slack elements is described and its effectiveness demonstrated. In particular an example of a diffused n-p junction is considered, with a variable bevel angle, and the results obtained are compared quantitatively with finite difference solutions. Due to its generality the technique can be employed in many device design applications and suggestions are made of the extension of this work to free surface profiles and device layout.

2. Introduction

Two-dimensional modelling of off-state semiconductor devices, under reverse-bias conditions, has been successfully achieved by many researchers using the finite element method of analysis [1,2]. This technique allows the accurate prediction of the device response through the numerical solution of the governing device equations and is generally applicable for a wide variety of device designs.

One of the most important device design considerations is correct surface termination. This is due to the adverse conditions that are inherent at the semiconductor surface. Neglecting this condition can result in surface breakdown at a considerably lower voltage than the possible bulk breakdown voltage value. A review of surface termination techniques has been presented by Baliga [3]. Here it is suggested that the peak surface field should be minimised to at least 50% of the bulk peak field value thereby encouraging bulk breakdown regardless of the unpredictable surface conditions.

The bevel angle surface termination technique enables conditions close to ideal bulk breakdown to occur. However this technique is limited to large surface area devices, typicaly 25 mm in diameter, and is uneconomical in the utilisation of disc area due to the shallow bevel angles required to achieve a significant reduction in the peak surface field. Other surface termination profiles have been devised, but until recently no serious attempt has been made to determine an optimum surface termination profile of arbitrary shape. The purpose of this paper is to show the feasibility of the objective proposed by the numerical testing of the optimisation algorithm on a single design variable problem which describes the shape of a bevelled p-n junction.

The device chosen for the study is a diffused n-p junction, which has been studied using finite differences by Gentry and Davies [4]. These co-workers give results for the change in peak surface field for a range of positive and negative bevel angles and the surface field profile is shown for various bevel angles. The device poses a "maximisation" problem as the peak surface field reaches a maximum for a negative bevel angle of approximately - 45 degrees. A quantitative comparison between the results given in reference [4] will be made with the proposed optimisation scheme developed by the authors.

3.1 The analysis model

The analysis model enables the solution of the governing device equations to be obtained, resulting in the determination of the potential and electric field distribution. It is used for the analysis of each new design case, or step, of the optimisation path and forms an integral part of the design model. The finite element program used for the analysis model is SWANOFF2 [2] which is described in depth by Waddell [5].

3.2 Finite element formulation of governing device equations

For semiconductor device modelling under reverse-bias, off state conditions, the usual approximation can be made to ignore the carrier transport equations as there is negligible current flow across the device. The potential distribution across a two-dimensional diode can therefore be expressed by the Poisson's equation (1) alone.

$$\frac{\partial^2\psi}{\partial x^2} + \frac{\partial^2\psi}{\partial y^2} = - \frac{\rho(\psi,x,y)}{k\varepsilon_0} \qquad (1)$$

The complete space charge equation given by expression (2) is incorporated in the finite element model thus enabling the accurate prediction of the potential ψ and electric field ε at

the depletion edges.

$$\rho(\psi,x,y) = q[(p + N_d) - (n + N_a)] \tag{2}$$

Here the strong dependency on ψ is found in the electron density n, and the hole density p, described by the usual Boltzmann's based equations. Implicit in the approximation above is that the quasi-fermi potentials ϕ_n for electrons and ϕ_p for holes, for each contacted region is a constant. The potential difference of the quasi-fermi potentials $(\phi_n - \phi_p)$ is considered to be equal to the reverse-bias V_e. The charge in the dielectric regions is assumed to be zero and therefore equation (1) reduces to the well known Euler equation

$$\kappa\varepsilon_0 \left(\frac{\partial^2\psi}{\partial x^2} + \frac{\partial^2\psi}{\partial y^2}\right) = 0 \tag{3}$$

It is also assumed that a zero surface charge exists along the bevel edge of the device.

A Galerkin weighted residual approach [6] is used in the formulation of the finite element expressions and the discretised equations (1)-(3) can be assembled in the usual matrix form as below

$$[C]\{\psi\} = \{Q(\psi)\} \tag{4}$$

here [C] is the constant capacitance matrix, $\{\psi\}$ is the potential vector, and $\{Q(\psi)\}$ is the highly non-linear charge vector.

4.1 The design model

The design model will be developed with the intention of determining a set of design variables which describe the surface termination profile. Optimisation will then consist of determining the set of design variables which minimise the peak surface electric field. The bevel angle junction termination is a special one variable case which enables the testing of the design optimisation algorithm. More importantly it also allows the accuracy of the design sensitivities to be determined.

4.2 Optimisation formulation

The general formulation for semiconductor device design optimisation can be presented in the classical form of a system objective function which is to be minimised subject to a set of applied constraints.

The discretised form of the optimisation problem can be written as

$$\text{Min } Z(\underline{x}) \equiv \min \varepsilon_q(\underline{x})_{max} \qquad q = 1, \ldots . p$$

subject to constraints (5)

$$g_r(\underline{x}) \leq 0 \qquad r = 1, \ldots m$$

where $\underline{x} = (x_1, \ldots x_n)^T$ is the design vector, the elements of which make up the set of design variables describing the position of the surface edge (shape). The vector $\varepsilon_q(\underline{x}) \equiv (\varepsilon_1, \ldots \varepsilon_p)$ is the discrete set of electric field values sampled at the centre of the surface elements in the silicon from which $\varepsilon_q(\underline{x})$ max is the maximum value. The functions $g_r(\underline{x}) \equiv (g_1(x) \ldots g_m(x))$ are a set of prescribed design constraints which are required to control the design process.

Many investigators seeking the solution to equations (5) have used sequential programming techniques with the objective and constraint functions being approximated by first order Taylor series. This approximation applied to equation (5) is defined as

$$\varepsilon_q(\underline{x}^k+\Delta\underline{x})_{max} \cong \varepsilon_q(\underline{x}^k)_{max} + \sum_{j=1}^{n} (\underline{x}_j-\underline{x}_j^k) \left(\frac{\partial \varepsilon_q}{\partial x_j} (\underline{x}^k)_{max}\right) \qquad (6)$$

and similarly

$$g_r(\underline{x}^k+\Delta\underline{x}) \cong g_r(\underline{x}^k) + \sum_{j=1}^{n} (\underline{x}_j-\underline{x}_j{}^k) \left(\frac{\partial g_r}{\partial x_j} (\underline{x}^k)\right) \qquad (7)$$

where $\underline{x}^k$ is the original design vector
$\underline{x}$ is the updated design vector
$\Delta\underline{x}_n$ is the change in the design vector
n is summation over the number of design variables

The unknown terms in these equations are the so-called design derivatives or design sensitivities

$$\frac{\partial \varepsilon_q}{\partial x_j} (x^k)_{max} \quad \text{and} \quad \frac{\partial g_r(\underline{x}^k)}{\partial x_j} \qquad (8)$$

and these must be calculated explicitly such that equations (6) and (7) can be described.

The accurate formulation of the design model is of prime importance since the sequential process used in the optimisation algorithm will require many resolutions of the non-linear device equations. Therefore it becomes mandatory that accurate and efficient techniques are adopted for the calculation of the design sensitivities.

4.3 Calculation of design derivatives

The numerical calculation of the design sensitivities for the non-linear equations (4) is achieved by the perturbation of the finite element mesh and then differencing the two solutions. For the bevel angle case, the angle θ is perturbated by amount γ which is preset to 10^{-3} degrees. The sensitivity calculation can be written as

$$\frac{\partial \varepsilon_q}{\partial \theta} (\theta)_{max} \cong \frac{\varepsilon_q(\theta^k+\gamma)_{max} - \varepsilon_q(\theta^k)_{max}}{\gamma} \qquad (9)$$

where $\varepsilon_q(\theta^k)$ is the maximum surface field value before perturbation

$\varepsilon_q(\theta^k+\gamma)$ is the maximum surface field value after perturbation

The sensitivity calculation procedure can be summarised by the following steps.

1. Converge the nonlinear finite element solution of equation (4) to a tolerance of 0.001%. This enables accurate electric field values to be determined.

2. Calculate the surface fields and find $\varepsilon_q(\theta^k)_{max}$. Store the maximum value of surface field and the Gauss point number at which it occurs.

3. Perturbate the original mesh by γ and reconverge equation (4) to the tolerance 0.001%. This normally requires 1 to 2 iterations when the perturbated mesh is initialised with the converged potentials of the original geometry.

4. Calculate the new value of $\varepsilon_q(\theta)$ at the previously stored Gauss point number.

5. Calculate the design sensitivity vector $\frac{\partial \varepsilon_q(\theta)}{\partial \theta}$ according to equation (9).

4.4 Mesh perturbation

An essential part of the design model is the mesh description which is used to redefine the device shape. Here mesh definition has a dual role in that it must permit both small and large coordinate changes to occur to allow both

sensitivity analysis and the resulting change in device geometry to take place. The grading of the mesh also requires consideration particularly at the surface edge between the two material regions where high potentials occur. To satisfy these requirements a specialised mesh perturbation technique has been developed which is related to the device problem and the type of finite element discretisation needed.

Although the procedure is demonstrated for the bevel angle surface termination method, it can also be used in a slightly modified form for general surface termination shapes.

Consider the mesh perturbation scheme shown diagramatically in Figure (1) Node 'P' is selected as a pivot positior and this lies on the surface edge at the end of the P-region contact plate. Element nodes located along AP and BC are fixed potential nodes with the correct bias of either zero or applied voltage respectively. Boundaries PEDC and AJB are natural boundary conditions. This implies that AJB the potential distribution within the bulk is one-dimensional and therefore $\frac{\partial \psi}{\partial x} = 0$.

When the mesh is perturbated by an amount θ each node except those located on AJB, DE and APE is moved horizontally by an increment $\Delta x_i = h_i \tan\theta$, where h_i is the vertical distance from any node i on the surface PNC to the y-ordinate of the pivot P. The x-ordinate of all nodes on the same y-ordinate as h_i are also adjusted by Δx_i and the procedure is repeated for each node located on PNC.

The advantage of this method of mesh redefinition is that mesh fineness and grading at the critical sampling positions remains unaltered. In fact the only change in mesh grading occurs in the "slack elements" on the boundaries of the discretised domain which maintains the natural boundary conditions at the edge of the mesh as prescribed. From resulting experience it was found that even at very large bevel angles there was negligible change in the potential values along AJB when compared with a value of $\theta = 0$. This confirms the resilience of the 4 noded linear element in maintaining the one dimensional solution within the bulk of the device even when subject to large distortions in shape.

4.5 The optimisation algorithm

Once the design sensitivity vector $\frac{\partial \varepsilon_q(\theta)_{max}}{\partial \theta}$ has been calculated, equations (5) can be explicitly described through equations (6) and (7) where n=1. A minimised solution may be found for this constrained problem but because of its linear nature it is immediately apparent that the model is only accurate for geometries in the vicinity of the original finite element mesh. In order to control this linear model and allow optimal solutions to be found it is necessary to apply a set of

additional constraints which in effect prevent sub-optimal solutions from entering a design space in which the design model is inaccurately defined.

These additional constraints or move limits restrict the step length taken from the current design vector θ^j and the *updated design vector* θ^{j+1}. *These limits can be incorporated* as an additional set of side constraints on the objective function as follows

$$\theta^j - \Delta\theta \leq \theta^{j+1} \leq \theta^j + \Delta\theta \qquad (10)$$

where $\Delta\theta$ is the prescribed allowable move limit.

The application of equation (10) sets up a restrictive design space which allows the linearised design model to be controlled between successive design steps. Figure 2 shows a schematic representation of the optimum design process for a device with a single design variable such as the bevel angle.

Furthermore the side constraints controlling the useable design space can be manipulated in order to increase the accuracy of the solution which is particularly important near the optimal where the design sensitivities approach a zero value. A flow diagram of the complete optimisation process is given in Figure 2. This flow diagram refers specifically to the *device mesh discussed in the previous section where the* design variable to be optimised is the device bevel angle. However the optimisation process can clearly be applied to many different device configurations with multiple design variables.

The optimisation process was initialised as shown in the flow diagram of Figure 3 and the change in bevel angle was limited to an absolute value of $\Delta\theta = 2$ between successive design steps. As convergence towards the maximum surface field is reached the move limits of equation (10) are reduced or re-tuned until the maximum value ε_{max} with respect to a small specified tolerance is satisfied. For each design step between 2 and 12 iterations were required for the resolution of the device governing equations. Here the number of iterations depend on the doping distribution across the device with the diffused junction usually requiring more iterations than the step junction. Resolution is also dependent on the surface field profile between the design steps and the magnitude of the sensitivities. For higher values of $\frac{\partial\varepsilon_{max}}{\partial\theta}$ a greater number of iterations would be required as the change in ε_{max} between succesive designs would be considerably increased.

The accuracy of the sensitivities calculated by the perturbation technique were shown to be excellent since the reduction in ε_{max} corresponds to within two significant figures

when compared with the value $\Delta\varepsilon_{max} = \frac{\partial\varepsilon_{max}\Delta\theta}{\Delta\theta}$, when $\frac{\partial^2\varepsilon_{max}}{\partial\theta^2}$ is small. This shows that the linearised objective function can accurately predict the change in ε_{max} for small changes in θ of the order of 2°. Hence the effectiveness of the optimal design process is demonstrated and the possibility of extending the method to the design of free-surface profile termination is apparent. For instance if the termination shape is determined by the nodal coordinates of a finite element mesh, then these nodes would form the set of design variables from which the surface field sensitivities could be calculated thus forming the design model to be optimised.

5. Silicon-diffused n-p junction example

The finite element mesh of the device to be investigated is shown in figure 4. The domain was discretised into 2121 linear quadrilateral elements with the mesh containing 2244 nodal points. "Slack elements" on both sides of the bevel surface allow both positive and negative bevel angles to be considered.

The material region in contact with the bevelled surface was assumed to be air with zero charge and a dielectric constant of k = 1.0 was assumed. In the p-type region the concentration of acceptor ions was $N_a = 2 \times 10^{14}$ atoms/cc and the diffused n-type silicon had a junction depth of 90 μm and an assumed complementary error function of donor density, $N_d = 8 \times 10^{18}$ atoms/cc at the surface. The complementary error function was calculated using the series expansion of reference [7] which allows the values of doping densities at the Gauss points within the n-region to be determined. These results were stored for subsequent use in calculating the charge at the Gauss points during the numerical integration phase. Doping densities were recalculated after each design step since the repositioning of the Gauss points in the diffused region produces a change in doping density values.

The locus of peak surface fields for the full range of complementary bevel angles is shown in figure 5. Again this is a plot of discrete values produced from sub-optimal designs and as seen the maximum peak surface field is located at θ = -49.5° shown in the figure at 90° -θ = -40.5°]. From reference [4] the maximum peak surface field is given as θ = -45° which compares well with the optimisation algorithm although there is some discrepancy in the values of peak maximum surface fields. This difference is attributed to the regular finite difference grid used by Davies and Gentry [4] and also to the fact that no account was taken in the finite difference formulation of the change in charge density of the grid points located adjacent to the surface in the silicon air region. For the finite element solution a fine mesh grading was used near the junction and bevel surface therefore allowing high surface fields to be predicted. Also in the finite element method the nodal

potential values were determined by numerical integration at the Gauss point positions of adjacent elements at the silicon air interface and therefore charge differences were explicitly taken into account. A section across the device when the complementary bevel angle is zero indicates that the increase in surface field from the bulk value occurs in a distance of only 1-2 microns from the surface edge. This behaviour demonstrates the necessity of fine mesh grading at the surface of the device to enable accurate sampling of the surface field.

It is considered that the agreement found in the bevel angle at the maximum peak surface field is due to the predominant effect of the area changes of the space charge region in determining the value of θ.

The surface field profiles across the bevelled surface are shown for various bevel angles in figure 6 and a contour plot of the maximum peak surface electric field is shown in figure 7 and the compression of the contour lines near the bevel surface are shown which produces the increase in surface field. Initial convergence of the potential distribution for $\theta = 90°$ was achieved after 504 cpu seconds and 76 iterations were required to satisfy a convergence tolerance of 0.001%. The complementary bevel angle range $\theta = 0-(-83°)$ required 3138 cpu seconds and the range $\theta = 0-(+84°)$ required 2350 cpu seconds which includes in each case over 40 redesigns and sub-optimised solutions. All calculations were carried out on a CDC CYBER 176.

6. Conclusions

This paper presents the development of a Design Model for the surface termination profile optimisation of semiconductor devices. The example described indicates that the finite element method is capable of predicting accurate device response and furthermore that a design model can be developed which is capable of optimising device response. The calculation of electric field sensitivities also proved to be inexpensive and accurate results were obtained. A mesh perturbation technique was developed incorporating "slack elements" and this has been shown to be suitable for the type of problems solved.

Surface electric fields for a diffused n-p device have been presented for various bevel angles and the maximum peak surface field has been predicted for a negative bevel angle. An optimisation model, using move limits and sequential redesign, has produced the accurate trace of the peak surface fields for a range of positive and negative bevel angles. These results effectively demonstrate that device response can be used to form accurate design models and furthermore that the possibility exists of producing optimal configurations for semiconductor devices [8].

It is possible to extend the concepts described herein to many different areas of device configurations with the aim of producing optimal device behaviour. For instance the investigation of free surfaces of arbitrary shape to obtain "optimum termination surfaces" is presently being undertaken by the authors. Many further possibilities exist where optimisation techniques could be used for device design such as material distribution, termination profile geometries and the inclusion of on-state device behaviour. These possibilities could prove to be invaluable to the designer since they promise to provide efficient and accurate designs thus replacing the time-consuming and difficult task of design via parametric studies.

References

1. W. L. ENGL, H. K. DIRKS and B. MEINERZHAGEN
   Device Modeling. Proceedings of the IEEE Vol. 71, No.1, pp. 10-33, 1983.

2. 'SWANOFF 2: A 2-dimensional off-state finite element package'. Department of Electrical and Electronic Engineering, University College of Swansea, Swansea, U.K.

3. B. J. BALIGA
   "High-voltage termination techniques - A comparative review", IEE Proceedings, Vol. 129, Pt. 1, No.5, pp. 173-179, 1982.

4. R. L. DAVIES and F. E. GENTRY
   "Control of electric field at the surface of P-N junctions". IEEE Trans., ED-11, pp. 313-323, 1964.

5. J. B. WADDELL
   "Numerical modelling by the F.E.M. of two dimensional semi-conductor devices under reverse-bias off-state conditions", M.Sc. Thesis, University of Wales, 1984.

6. E. HINTON and D. R. J. OWEN
   "An introduction to Finite Element Computations". Pineridge Press, 1979.

7. Handbook of Mathematical Functions. Edited by M. Abramowitz and I. A. Segun. Dover Publications, 1964.

8. SEMIOPT, MK1, "Optimization of free surface termination profiles", Finite element off state numerical package. Department of Civil Engineering, University College of Swansea, Swansea, U.K.

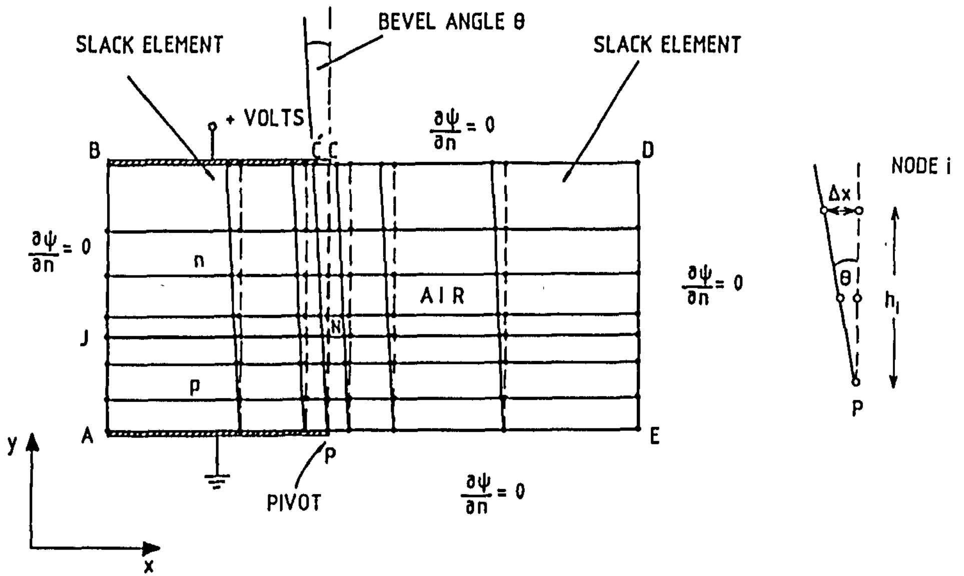

Fig. 1 Mesh perturbation technique incorporating slack elements to maintain constant grading and natural boundary conditions. Each free node is perturbated by $\Delta x_i = h_i \tan\theta$, where h_i is the vertical distance from node i to P.

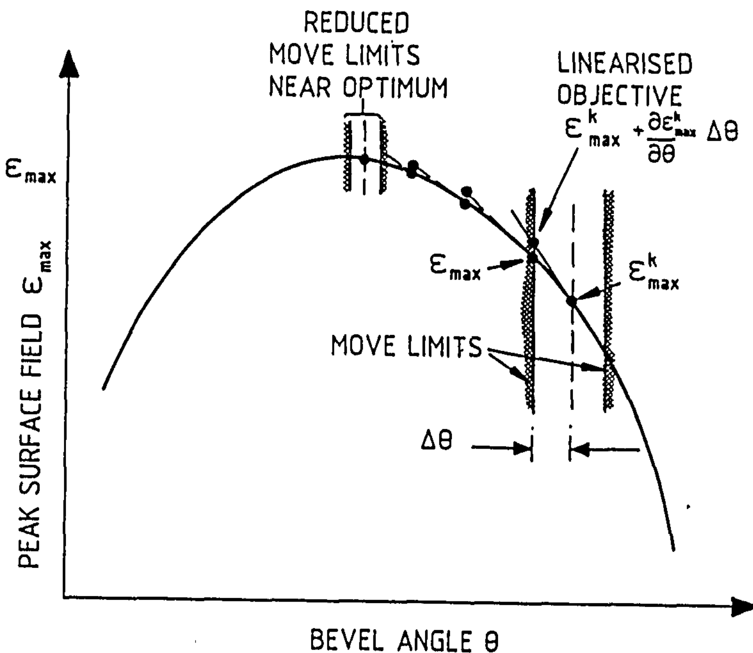

Fig. 2 Sub-optimal design steps using a linear objective function and adjustable move limits which reduce on approaching the "optimum" design.

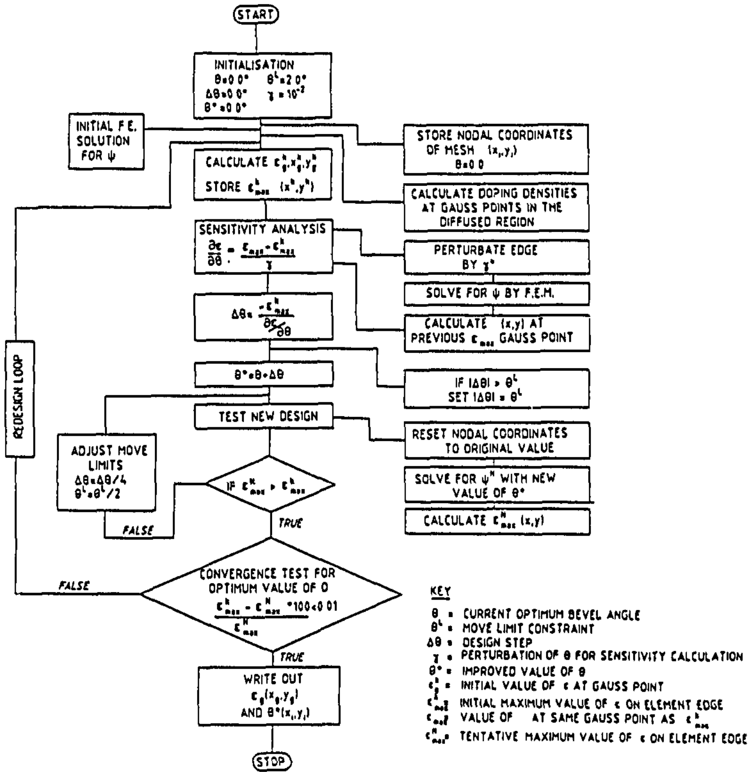

Fig. 3 Flow chart of optimisation algorithm for bevelled p-n junctions.

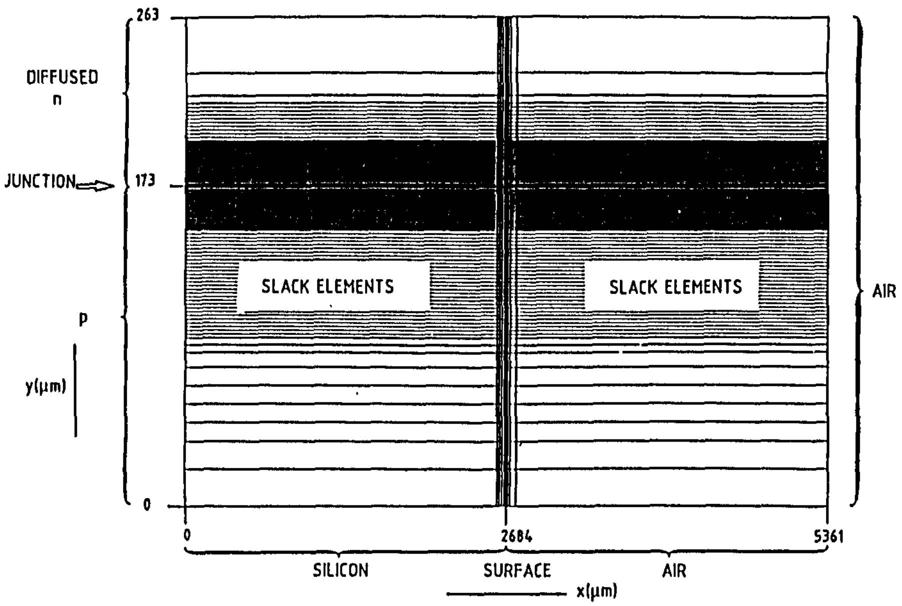

Fig. 4 Finite element mesh for diffused n-p function. Device discretised into 2121 linear quadrilateral elements. A complementary error was used to define the doping profile in the n region, with a junction depth of 90 μm and surface doping density of

$N_d = 8 \times 10^{18}$ atoms/cc. In the p region

$N_a = 2 \times 10^{14}$ atoms/cc. The dielectric constant

κ for air assumed to be unity.

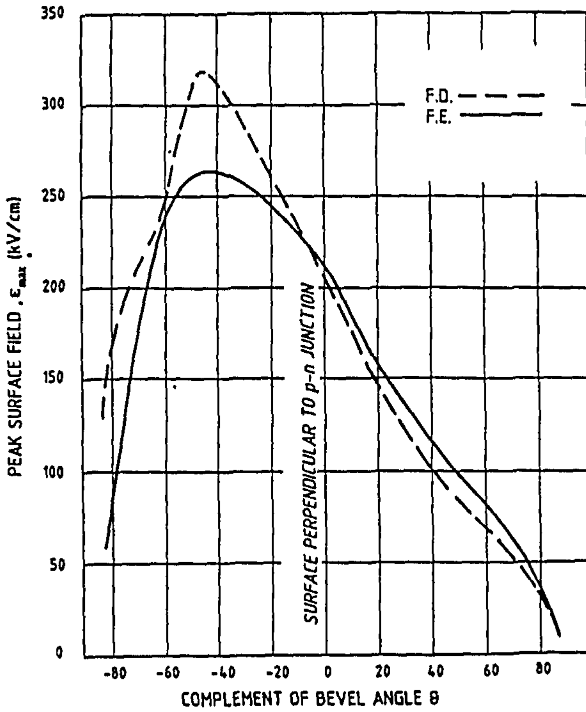

Fig. 5 Relationship between peak surface field and bevel angle θ for positive and negative bevelled diffused n-p junction of Fig. 4. Finite element results (F.E.) and Davies and Gentry [4] results (F.D.).

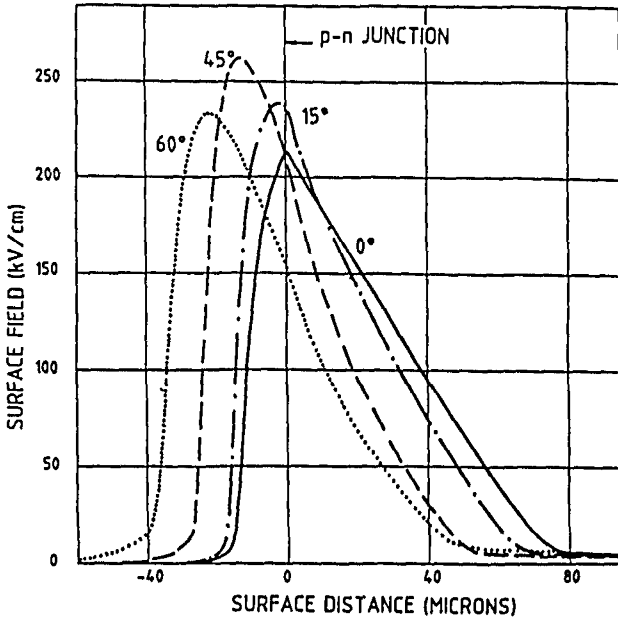

Fig. 6 Surface field profiles along the bevelled surface for various negative bevel angles of the diffused n-p junction of Fig. 4.

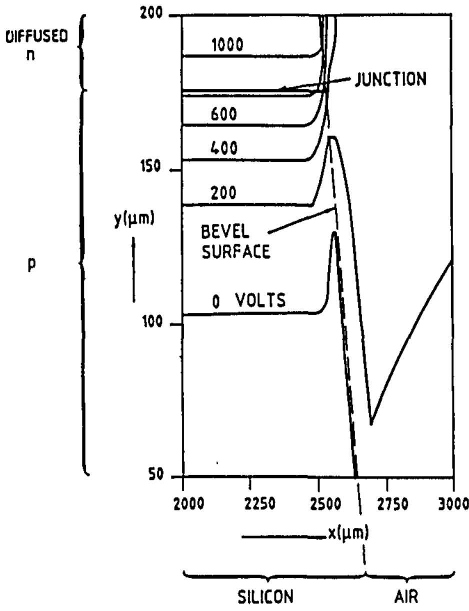

Fig. 7 Solution of the potential distribution across the diffused n-p junction of Fig. 4, at the maximum peak surface field ε_{max}. The negative bevel angle $\theta = -49.5°$ or $-40.5°$ as shown in Fig. 5.